Title

POLE EXTRAPOLATION OP THE REACTIONS n-p ---> n-n+ AND n+p --> n+n- (1238)

Authors

Colton, Eugene
Malamud, Ernest.

Publication Date

1971

Submitted to Physical Review

POLE EXTRAPOLATION OF THE REACTIONS $\pi^- p \to \pi^- \pi^+ n$ AND $\pi^+ p \to \pi^+ \pi^- \Delta^{++}(1238)$

Eugene Colton and Ernest Malamud

January 1971

AEC Contract No. W-7405-eng-48

LAWRENCE RADIATION LABORATORY
UNIVERSITY of CALIFORNIA BERKELEY

POLE EXTRAPOLATION OF THE REACTIONS $\pi^- p \to \pi^- \pi^+ n$ and $\pi^+ p \to \pi^+ \pi^- \Delta^{++}$ (1238)*

Eugene Colton

Lawrence Radiation Laboratory
University of California
Berkeley, California 94720

and

Ernest Malamud

National Accelerator Laboratory
Batavia, Illinois 60510

ABSTRACT

Experimental differential cross-sections from data on the reactions $\pi^- p \to \pi^- \pi^+ n$ and $\pi^+ p \to \pi^+ \pi^- \Delta^{++}$ (1238) have been extrapolated to the one-pion-exchange pole to obtain the $\pi^+ \pi^-$ elastic scattering cross section from threshold to 1.4 GeV. Consistent results are obtained in three c.m. energy ranges for both reactions. The data have been fit to several t-dependent extrapolation functions, and the results of the fits are tabulated and plotted as a function of $\pi^+ \pi^-$ effective mass. In particular, we find cross sections of approximately 25 and 125 mb, respectively, at the K and central $\rho^0(765)$ mass positions.

I. INTRODUCTION

The proper extraction of $X\pi$ elastic scattering cross sections from data on the reactions $Xp \to X\pi^+ n$ and $Xp \to X\pi^- \Delta^{++}(1238)$ [for $X = \pi$, K, p] has been the goal of many experiments since the work of Goebel,[1] and Chew and Low.[1] Many analyses, which include the fits of experimental differential cross sections to various theoretical formulas as well as numerous extrapolation procedures, have either assumed or attempted to show that single-pion exchange is dominant in the above reactions in the intermediate energy region. More recently, however, Kane[2] has pointed out that other exchanges (e.g., ρ, A2) are just as, if not more, important in the region of small momentum transfer. Thus it appears that if pion-exchange is indeed present in a reaction, an appropriate extrapolation procedure must be carried out in order to isolate and determine its magnitude.

In this paper we present a determination of the $\pi^+\pi^-$ elastic scattering cross section by means of a modified Chew-Low[1] extrapolation to the pion-exchange pole in the reactions

$$\pi^- p \rightarrow (\pi^-\pi^+)n \qquad (1a)$$

and

$$\pi^+ p \rightarrow (\pi^+\pi^-)\,\Delta^{++}\,(1238) \qquad (1b)$$

We assume (for small momentum transfer) that the processes depicted in Figs. 1(a) and 1(b) play significant roles in reactions (1a) and (1b), respectively. The extrapolation procedure which we use has been shown[3] to successfully yield π^+p elastic scattering cross sections in the region of the $\Delta^{++}(1238)$ resonance from peripheral data on the reaction $pp \rightarrow (p\pi^+)n$ at 6.6 GeV/c incident laboratory beam momentum. The method involves first normalizing the experimental differential cross section $(d\sigma/dt)_{exp.}$ at $\pi^+\pi^-$ effective mass m, to a function which behaves similarly with t, but which reduces to the required value at the pion-exchange pole. The normalized data points are then fit to a low-order polynomial in t. The pole value of the polynomial with best fit parameters yields the $\pi^+\pi^-$ elastic scattering cross section. The procedure does not require extrapolation of quantities with poles and does not require the pion-exchange cross section to vanish at zero momentum transfer in the data of reaction (1a). Effects such as helicity dependence, absorption, and Reggeization of the exchanged pion as thus allowed for.

In Sec. II we list and examine the data used in the extrapolation. The extrapolation procedure and the fits to the data are discussed in Secs. III and IV, respectively. The results and conclusions are put forth in Sec. V.

II. EXPERIMENTAL DATA

The analysis of the data[4] of reaction (1a) has been performed upon a total of 20,541 events which have been subdivided into 5082, 7728, and 7731 events corresponding to intervals in center of mass energy of 2.0 - 2.37, 2.37 - 2.49, and 2.49 - 2.70 GeV, respectively. The analysis of the data[5] for reaction (1b) has been performed upon a total of 17,729 events of the type

$$\pi^+ p \rightarrow \pi^+\pi^-\pi^+ p \qquad (2)$$

which are subdivided into 7207, 4653, and 5869 events corresponding to three intervals in c.m. energy. The first two intervals occupy ranges of 2.57 - 2.78, and 2.78 - 2.98 GeV in c.m. energy and the third interval contains events with nominal beam momenta of 6.94 (3.73 GeV c.m.) and 8.4 (4.08 GeV c.m.) GeV/c. For the purpose of further discussion we denote the separation of events into c.m. energy intervals as experiments, characterized by the ordinal numbers 1, 2, and 3.

The strong Δ^{++} (1238) component in reaction (2) can be seen in the histograms of π^+p effective mass in Figs. 2(a) - 2(c) (corresponding to the three experiments). Two combinations are plotted for each event. In order to obtain events corresponding to reaction (1b) we require

$$1.12 < M < 1.34 \text{ GeV} \tag{3}$$

where M is the π^+p effective mass. If both M combinations for an event fall within the cut (3) then we use that combination with the smaller value of t measured from the target proton to that outgoing Δ^{++} (1238) combination. The four-momentum transfer squared (t) is chosen to be positive in the physical region. The $\pi^+\pi^-$ effective mass spectra for reactions (1a) and (1b) are presented in Figs. 3 and 4, respectively. The presence of ρ^0(765) production is obvious. Additional structure near 1250 MeV for the higher c.m. energy experiments is evidence for f^0(1260) resonance production.

III. EXTRAPOLATION PROCEDURE

The experimental $d\sigma/dt$ for reactions (1a) and (1b) have been extrapolated to the one-pion-exchange pole for different $\pi^+\pi^-$ mass regions (for each experiment) following the procedure of Ma et al.[3] This procedure differs from the traditional Chew-Low method in that the experimental differential cross section $(d\sigma/dt)_{exp.}$ is normalized to the pole equation modified by a suitable form factor, instead of to the pole equation alone. For reactions (1a) and (1b) we write[6]

$$\frac{d^2\sigma}{dt\,dm} = \frac{1}{4\pi m_p^2 P_L^2} \frac{g^2}{4\pi} \frac{t}{(t+\mu^2)^2} [m^2 q(m)\sigma(m)] F(m,t) \tag{4a}$$

and

$$\frac{d^3\sigma}{dt\,dm\,dM} = \frac{1}{4\pi^3 m_p^2 P_L^2} \frac{[m^2 q(m)\sigma(m)]}{(\hbar c)^2} \frac{[M^2 Q(M)\sigma(M)]}{(t+\mu^2)^2} F(m,M,t) \qquad (4b)$$

respectively. In Eqs. (4) $\mu(m_p)$ are the pion (proton) rest masses, P_L is the laboratory beam momentum, $g^2/4\pi = 29.2$, m(M) are the $\pi^+\pi^-(\pi^+p)$ effective masses, q(Q) are the momenta in the $\pi^+\pi^-(\pi^+p)$ rest systems, and the σ functions are the on-mass-shell vertex elastic scattering cross sections. All quantities have the units GeV or mb, except F which is dimensionless.

The form factors (F) used in Eqs. (4) can be any smooth continuous functions which reduce to unity at the pion-exchange pole. To obtain suitable F functions we first multiply the phenomenological Dürr-Pilkuhn[7] (referred to hereafter as DP) $\rho^0(765)$ vertex factor by the t dependent form factor[8] which Wolf[9] found was necessary in order to describe the t distributions of various quasi-two-body processes. Defining a function G we write

$$G(m,t) = \left[\frac{2.3-\mu^2}{2.3+t}\right]^2 \left(\frac{q_t}{q}\right)^2 \left[\frac{1+(8.3q)^2}{1+(8.3q_t)^2}\right] \qquad (5)$$

where q_t is the momentum of the incoming beam pion evaluated in the $\pi^+\pi^-$ rest system. The form factor appearing in Eq. (4a) is given by

$$F(m,t) = \left[\frac{1+7.1(q_n)^2}{1+7.1(q_n)_t^2}\right] G(m,t) \qquad (6a)$$

where $(q_n)_t^2$ is the momentum squared of the incoming target proton evaluated in the neutron rest system, and $(q_n)^2$ is this quantity taken on-shell. Similarly the form factor appearing in Eq. (4b) is given by the product of the phenomenological DP Δ^{++} (1238) vertex factor and G(m,t):

$$F(m,M,t) = \left(\frac{Q_t}{Q}\right)^2 \left[\frac{1+(4Q)^2}{1+(4Q_t)^2}\right] \left[\frac{(M+m_p)^2+t}{(M+m_p)^2-\mu^2}\right] G(m,t) \qquad (6b)$$

where Q_t is the momentum of the incoming target proton evaluated in the Δ^{++} rest system. The use of form factors such as (6a) and (6b) along with other appropriate Dürr-Pilkuhn factors have been shown[9,10] to describe experimental Chew-Low distributions for strong-interaction reactions of the classes $Xp \to X\pi^+ n$ and $Xp \to X\pi^- \Delta^{++}$ (for $X = \pi, K, p$) over a large range of beam momenta. The usefulness of this procedure lies in the fact that the complexity of the t-dependence of the function to be extrapolated is minimized, thereby decreasing the order of the polynomial which is fit to the experimental points.

The functions which we extrapolate to the pole for each specified interval in $\pi^+\pi^-$ mass (Δm) are

$$"t\sigma" = \frac{(d\sigma/dt)_{exp.}}{(1/t)(d\sigma/dt)_{DP\text{-}OPE}} \tag{7a}$$

for reaction (1a) and

$$"\sigma" = \frac{(d\sigma/dt)_{exp.}}{(d\sigma/dt)_{DP\text{-}OPE}} \tag{7b}$$

for reaction (1b). The expressions $(d\sigma/dt)_{DP\text{-}OPE}$ in Eqs. (7a) and (7b) are Eqs. (4a) and (4b), respectively, after integration over the variable(s) other than t. The on-shell cross sections $\sigma(m)$ are set equal to 1 mb in calculating the denominator so that at the pole $-\mu^2\sigma^{\pi^+\pi^-}_{on\text{-}shell}$ ="$t\sigma$" and $\sigma^{\pi^+\pi^-}_{on\text{-}shell}$ = "σ" for reactions (1a) and (1b), respectively. Polynomials in t are then fit to the experimental "$t\sigma$" and "σ" points. Note that if $(d\sigma/dt)_{DP\text{-}OPE}$ has precisely the same t dependence as $(d\sigma/dt)_{exp.}$ then "$t\sigma$" points can be described by the form bt and "σ" points are independent of t. Thus the need for other terms in the polynomial expressions allows for departure of $(d\sigma/dt)_{DP\text{-}OPE}$ from $(d\sigma/dt)_{exp.}$

IV. FITS TO DATA

The experimental "$t\sigma$" values for reaction (1a), calculated[11] using Eq. (7a), are displayed in Figs. 5 - 7. The three figures are subdivided into 11, 13, and 13 parts corresponding to the denoted regions of $\pi^+\pi^-$ effective mass, respectively. Least-squares fits of the data in Figs. 5 - 7 have been performed separately to the assumed forms $a + bt$, bt, and $bt + ct^2$. The resulting confidence levels and the best fit values of the parameters, as well as the extrapolated on-mass-shell $\pi^+\pi^-$ elastic scattering cross sections are presented in Tables I - III. The numbers listed in the second column of the tables represent only the peripheral (small t) events used to calculate the experimental "$t\sigma$" points. All of the fits listed in the tables have acceptable confidence levels ($\geq 1\%$) except for the "$t\sigma$" = bt fit in the lowest $\pi^+\pi^-$ mass range in Table I. Therefore the experimental differential cross sections $(d\sigma/dt)_{exp.}$ appear to be adequately represented by $(d\sigma/dt)_{DP-OPE}$ in the t and m ranges considered here. The straight lines and the extrapolated points at $t = -\mu^2$ (in Figs. 5 - 7) represent the expansion "$t\sigma$" = a + bt using for a and b the best fit values obtained in the least-squares fits. Tables I - III indicate that the a and c parameters obtained in the fits are generally consistent with zero. However, they are negative and positive, respectively, in the central ρ mass region. Thus, the resulting extrapolated cross sections from the a + bt and bt + ct^2 fits are larger and smaller than the bt fit value, respectively, in the central ρ mass region. The extrapolated cross sections listed in Tables I - III are plotted in Figs. 8(a) - 8(c) as a function of $\pi^+\pi^-$ effective mass. The smooth curves drawn in Fig. 8 are $12\pi\lambda^2$ which represent the unitarity limit for an elastic p-wave $\pi\pi$ resonance. The points in Figs. 8(a), 8(b), and 8(c) occur below, above, and below the unitarity limit at the ρ mass peak, respectively.

The experimental "σ" points for reaction (1b), calculated[12] using Eq. (7b), are displayed in Figs. 9 - 11. The three figures are subdivided into 12, 9, and 10 parts corresponding to the denoted regions of $\pi^+\pi^-$ effective mass, respectively. Least-squares fits of the data in Figs. 9 - 11 have been performed separately to the assumed forms a and a + bt. The resulting confidence levels and the best fit values of the parameters, as well as the extrapolated on-mass-shell $\pi^+\pi^-$ elastic scattering cross sections, are presented in Tables IV - VI. As above, the numbers listed in column 2 of each table represent only the peripheral events used to calculate the experimental "σ" points. Five of the "σ" = a fits listed in Tables IV - VI have unacceptable confidence levels ($< 1\%$). In the remaining cases, however, the experimental differential cross sections $(d\sigma/dt)_{exp.}$

appear to be adequately described by $(d\sigma/dt)_{DP-OPE}$ in the t and m ranges considered. The straight lines and the extrapolated cross sections at $t = -\mu^2$ (in Figs. 9 - 11) represent the expansion "σ" = a + bt using for a and b the best fit values obtained in the least-squares fits. Figures 9 - 11 indicate an abrupt change in slope parameter b while passing through the ρ region. The change from positive to negative values of b accounts for the large values of extrapolated cross section observed in the $\pi^+\pi^-$ mass bin starting at 0.78 GeV. The extrapolated cross sections listed in Tables IV - VI are displayed in Figs. 12(a) and 12(b) as a function of $\pi^+\pi^-$ effective mass. The smooth curves drawn in Fig. 12, again represent the p-wave unitarity limit. The points in both Figs. 12(a) and 12(b) exceed the unitarity limit at the ρ mass peak.

V. DISCUSSION AND CONCLUSIONS

The extrapolated $\pi^+\pi^-$ elastic scattering cross sections resulting from the different fits appear to be similar for the three experiments in all cases. This observation supports the one-pion-exchange hypothesis and indicates that the systematic effects induced by errors in the experimentally determined cross sections for reactions (1a) and (1b) are small compared to the statistical errors. In Table VII we list the extrapolated cross sections, averaged over the three experiments, from both reactions (1a) and (1b). These cross sections are also plotted in Figs. 13(a) and 13(b), respectively, as a function of $\pi^+\pi^-$ mass. The cross sections obtained from each of the assumed forms for "$t\sigma$" and "σ" appear to be quantitatively consistent everywhere except in the central ρ mass region. In particular, a value of roughly 25 mb is observed at the K mass. In the central ρ mass bin the "$t\sigma$" = a + bt and "σ" fits indicate an average cross section of roughly 125 mb. The "$t\sigma$" = bt and "$t\sigma$" = bt + ct^2 fits yield cross sections which are somewhat smaller at the ρ mass peak. The latter effect has also been observed in an earlier analysis by Marateck et al.[13] One expects a significant s-wave contribution[14] at 0.765 GeV so the results of our "$t\sigma$" = a +bt fits are probably more reliable.[15] Each of the fits indicate a ρ width (FWHM) of around 150 MeV. However the unknown resolution inherent in data compilations such as these prevents an accurate estimation. Presumably a value such as 130 MeV would be consistent with our results.

The curves appearing in Fig. 13 were calculated from the theoretical expression for σ

$$\sigma = 4\pi\lambda\!\!\!^{-2}\left[3\sin^2\delta_1^1 + \frac{1}{9}\left\{\sin^2\delta_0^2 + 4\sin^2\delta_0^0 + 4\cos(\delta_0^2-\delta_0^0)\sin\delta_0^2\sin\delta_0^0\right\}\right] \quad (8)$$

where δ_L^T is the scattering phase shift for angular momentum L and I-spin T, and only s and p-wave $\pi^+\pi^-$ elastic scattering are assumed to occur. In Eq. (8) $\sin^2\delta_1^1$ was taken to be a resonant p-wave Breit-Wigner of mass and width 0.765 and 0.125 GeV, and the values for the s-wave phase shifts δ_0^2 and δ_0^0 were obtained from the analyses of Colton et al.[16] and Malamud et al.,[17] respectively. The solid and dashed curves correspond to using the "up-up" and "up-down" solutions for δ_0^0, respectively, in Eq. (8). Both curves agree with the averaged extrapolated cross sections below the central ρ region in both Figs. 13(a) and 13(b). Above 0.8 GeV the dashed curve appears to agree more closely with the averaged extrapolated cross sections. The data in Figs. 13(a) and 13(b) have also been compared to the predictions of Eq. (8) using for δ_0^0 the "down-up" solutions of both Malamud et al.[17] and Marateck et al.[13] While reasonably good agreement between the data and predictions is observed in the ρ region and above, poor agreement (predicted σ too low) is observed below $m = 0.65$ GeV.

In conclusion we have performed an extrapolation to the pion-exchange-pole in reactions (1a) and (1b) in three c.m. energy regions in order to determine the $\pi^+\pi^-$ elastic scattering cross section for $\pi^+\pi^-$ effective masses below 1.4 GeV. The pole extrapolation performed here differs from earlier methods[13] in that: (a) We first normalize the experimental differential cross section to the pole-equation modified by appropriate form factors instead of to the pole equation alone; (b) in the analysis of the data for reaction (1a) we allow for non-vanishing contributions of the experimental differential cross section (e.g., "tσ") at t = 0 in our fitting procedure. The results of using several t-dependent extrapolation functions to fit the data of reaction (1a) are somewhat ambiguous in that generally good fits are obtained to the "$t\sigma$" points, but the extrapolated $\pi^+\pi^-$ elastic scattering cross sections differ somewhat at the ρ-mass peak. Clearly an order of magnitude increase in the number of available $\pi^- p \to \pi^-\pi^+ n$ events is necessary in order to accurately determine the a and c parameters in the $a + bt + ct^2$ fits to "$t\sigma$" points which are evidently required for a more precise extrapolation.

We find, additionally, that the extrapolated $\pi^+\pi^-$ elastic scattering cross sections obtained using each extrapolation function are similar for each c.m. energy region. The c.m. energy averaged results of reaction (1b) and the $a + bt$ fit results of reaction (1a) are consistent with each other and with those values obtained from the plane-wave expansion for σ [Eq. (8)], which utilizes published values for the s-wave phase shifts.

We thank Professor Peter E. Schlein for helpful suggestions.

REFERENCES AND FOOTNOTES

* Supported in part by the United States Atomic Energy Commission.

1. C. Goebel, Phys. Rev. Letters 1, 337 (1958).
   G. F. Chew and F. E. Low, Phys. Rev. 113, 1640 (1959).
2. G. L. Kane, Experimental Meson Spectroscopy 1970, Eds. C. Bartay and A. H. Rosenfeld (Columbia University Press - 1971) p. 1.
3. Z. Ming Ma et al., Phys. Rev. Letters 23, 342 (1969). For additional description of the pole extrapolation procedure see e.g., E. Colton and P. E. Schlein in The Proceedings of the Conference on $\pi\pi$ and $K\pi$ Interactions, Argonne National Laboratory, May 14-16, 1969, p. 1.
4. The following laboratories and collaborations have generously contributed their data on the reaction $\pi^- p \to \pi^- \pi^+ n$. Pennsylvania-Saclay-Orsay- Bari-Bologna [V. Hagopian et al., Phys. Rev. 145, 1128 (1966); Y. Pan, Phys. Rev. 152, 1183 (1966)]. Purdue [D. H. Miller et al., Phys. Rev. 153, 1423 (1967)]. Lawrence Radiation Laboratory [L. Jacobs, Lawrence Radiation Laboratory report UCRL-16877 (1966)]. Argonne-Toronto-Wisconsin [D. R. Clear et al., Nuovo Cimento 49A, 399 (1967); A. W. Key, et al., Phys. Rev. 166, 1430 (1968)].
5. The following laboratories and collaborations have generously contributed their data on the reaction $\pi^+ p \to \pi^+ \pi^- \pi^+ p$. Rochester-Yale [P. Slattery, H. Kraybill, B. Forman, and T. Ferbel, University of Rochester report UR-857-153 (1966)]. Lawrence Radiation Laboratory [D. Brown et al., Lawrence Radiation Laboratory report UCRL-17665 (1967); D. Brown, Lawrence Radiation Laboratory report UCRL-18254 (1968)]. Lawrence Radiation Laboratory [G. Goldhaber et al., Phys. Rev. Letters 12, 336 (1964)]. University of California, San Diego [Maris Abolins et al., Phys. Rev. Letters 11, 381 (1963)]. Columbia-Rutgers [M. Rabin, R. Plano, C. Baltay, P. Franzini, L. Kirsch, H. Kung, and N. Yeh, Bull. Am. Phys. Soc. 12, 9 (1967)].
6. See e.g., E. Ferrari and F. Selleri, Supp. Nuovo Cimento 24, 453 (1962).
7. H. P. Dürr and H. Pilkuhn, Nuovo Cimento 40, 899 (1965).
8. G. Goldhaber et al., Physics Letters 6, 62 (1963).
9. G. Wolf, Phys. Rev. Letters 19, 925 (1967).

10. P. Schlein in The Proceedings of The Conference on $\pi\pi$ and $K\pi$ Interactions, Argonne National Laboratory, May 14-16, 1969, pps. 1 and 446. See also Review talk by P. Schlein at the Informal Meeting on Experimental Meson Spectroscopy, University of Pennsylvania, April 26-27, 1968. Published in Meson Spectroscopy, ed. C. Baltay and A. H. Rosenfeld (W. A. Benjamin, Inc., 1968), p. 161.

11. We use the expression

$$"t\sigma" = \frac{c}{\int dt\ dm} \sum_{i=1}^{N} \left[\frac{t}{(d^2\sigma/dt\ dm)_{DP\text{-}OPE}}\right]_i$$

to evaluate "$t\sigma$" for a given $\Delta t \Delta m$ bin. Here c is the mb/event factor, the sum is over the events in the sample, and the bracketed quantity is evaluated for each event. The integral $\int$ dtdm is over that portion of the $\Delta t \Delta m$ in question which is included in the physical region of the Chew-Low plot.

12. We use the expression

$$"\sigma" = \frac{c}{\int dt\ dm\ dM} \sum_{i=1}^{N} \left[\frac{1}{(d^3\sigma/dt\ dm\ dM)_{DP\text{-}OPE}}\right]_i$$

to evaluate "σ" for a given $\Delta t\ \Delta m\ \Delta M$ bin. The other quantities are defined in Ref. 10.

13. S. Marateck et al., Phys. Rev. Letters 21, 1613 (1968).

14. D. Morgan and G. Shaw, Phys. Rev. D2, 520 (1970).

15. Other independent work also demonstrates the presence of a non-zero component in the experimental differential cross section (e.g., "$t\sigma$") for transverse ρ production at $t = 0$. The precision of this analysis is unable to positively verify this observation, although it does suggest a negative value.
See e.g., A. Boyarski et al., Phys. Rev. Letters 20, 300 (1968); R. Diebold and J. Poirier, ibid 20, 1552 (1968).

16. E. Colton et al., Lawrence Radiation Laboratory report UCRL-20053 submitted to the XVth International Conference on High Energy Physics, Kiev, U.S.S.R. (August 27-September 4, 1970).

17. E. Malamud and P. E. Schlein in The Proceedings of the Conference on ππ and Kπ Interactions, Argonne National Laboratory, May 14-16, 1969, p. 93.

Table I. Results of fits of the "$t\sigma$" data points, for Experiment 1 in $\pi^- p \rightarrow (\pi^-\pi^+)n$, to the assumed forms $a + bt$, bt, and $bt + ct^2$.

		"$t\sigma$" = a + bt			"$t\sigma$" = bt		"$t\sigma$" = bt + ct^2		
$\pi^+\pi^-$ Mass Range (GeV)	Events	σ (mb)	a/μ^2 (mb)	Prob. (%)	σ (mb)	Prob. (%)	σ (mb)	$c\mu^2$ (mb)	Prob. (%)
.28-.46	56	47 ± 13	-20 ± 8	2	14 ± 2	< 1	3 ± 4	3 ± 1	22
.46-.54	70	48 ± 19	- 9 ± 12	2	33 ± 4	4	15 ± 10	5 ± 3	8
.54-.62	104	46 ± 12	- 9 ± 8	92	32 ± 3	65	27 ± 6	1 ± 1	68
.62-.68	159	46 ± 18	2 ± 13	94	49 ± 4	99	49 ± 8	0 ± 1	93
.68-.72	261	64 ± 31	22 ± 22	13	95 ± 6	15	100 ± 13	-1 ± 2	8
.72-.75	225	122 ± 44	-11 ± 31	11	107 ± 7	18	107 ± 17	0 ± 3	11
.75-.78	297	140 ± 47	-21 ± 35	1	112 ± 7	2	86 ± 15	5 ± 2	5
.78-.81	267	167 ± 50	-55 ± 38	1	96 ± 6	1	70 ± 13	5 ± 2	4
.81-.85	215	70 ± 39	- 7 ± 31	96	61 ± 4	92	56 ± 11	1 ± 2	89
.85-.90	200	77 ± 37	-26 ± 30	82	44 ± 3	78	36 ± 9	1 ± 1	88
.90-.98	209	-34 ± 38	53 ± 32	13	29 ± 2	7	34 ± 7	-1 ± 1	4

Table II. Results of fits of the "tσ" data points, for Experiment 2 in $\pi^- p \rightarrow (\pi^-\pi^+)n$, to the assumed forms a + bt, bt, and bt + ct^2.

		"tσ" = a + bt			"tσ" = bt		"tσ" = bt + ct^2		
$\pi^+\pi^-$ Mass Range (GeV)	Events	σ (mb)	a/μ^2 (mb)	Prob. (%)	σ (mb)	Prob. (%)	σ (mb)	$c\mu^2$ (mb)	Prob. (%)
.28- .46	53	35 ± 11	-14 ± 7	20	14 ± 2	6	6 ± 4	2 ± 1	80
.46- .54	65	12 ± 11	7 ± 7	65	24 ± 3	52	28 ± 7	-1 ± 1	36
.54- .62	139	47 ± 10	- 9 ± 6	72	32 ± 3	33	25 ± 5	2 ± 1	66
.62- .68	226	46 ± 12	3 ± 7	88	50 ± 3	94	50 ± 7	0 ± 1	85
.68- .72	300	95 ± 19	- 7 ± 12	78	85 ± 5	83	81 ± 11	1 ± 2	76
.72- .75	331	103 ± 26	5 ± 18	23	110 ± 6	31	111 ± 14	0 ± 3	22
.75- .78	418	144 ± 26	-24 ± 18	2	110 ± 6	2	80 ± 11	6 ± 2	28
.78- .81	418	128 ± 26	-18 ± 18	37	104 ± 5	37	95 ± 10	2 ± 2	38
.81- .85	370	97 ± 21	-23 ± 15	42	65 ± 3	28	54 ± 7	2 ± 1	52
.85- .90	323	46 ± 18	- 3 ± 14	10	41 ± 2	16	33 ± 6	2 ± 1	23
.90- .98	343	55 ± 13	-24 ± 10	71	24 ± 1	20	17 ± 3	1 ± 0	95
.98-1.1	252	30 ± 12	-16 ± 10	8	12 ± 1	7	7 ± 2	1 ± 0	26
1.1 -1.2	251	40 ± 25	-22 ± 22	88	15 ± 1	82	11 ± 3	0 ± 0	96

Table III. Results of fits of the "tσ" data points, for Experiment 3 in $\pi^- p \rightarrow (\pi^- \pi^+)n$, to the assumed forms a + bt, bt, and bt + ct^2.

		"tσ" = a + bt			"tσ" = bt		"tσ" = bt + ct^2		
$\pi^+\pi^-$ Mass Range (GeV)	Events	σ (mb)	a/μ^2 (mb)	Prob. (%)	σ (mb)	Prob. (%)	σ (mb)	cμ^2 (mb)	Prob. (%)
.46- .54	66	30 ± 13	- 2 ± 8	89	26 ± 3	95	25 ± 7	0 ± 2	80
.54- .62	110	41 ± 13	- 6 ± 8	26	31 ± 3	40	22 ± 8	3 ± 2	50
.62- .68	173	28 ± 12	7 ± 8	5	40 ± 3	8	36 ± 7	1 ± 2	3
.68- .72	212	70 ± 17	- 5 ± 11	68	62 ± 4	78	57 ± 10	1 ± 2	72
.72- .75	320	101 ± 21	- 2 ± 13	81	98 ± 6	90	103 ± 11	-1 ± 2	86
.75- .78	415	121 ± 23	- 6 ± 15	60	112 ± 6	67	111 ± 11	0 ± 2	58
.78- .81	368	96 ± 23	- 3 ± 15	27	92 ± 5	37	84 ± 10	2 ± 2	35
.81- .85	405	55 ± 15	5 ± 11	35	63 ± 3	42	67 ± 6	-1 ± 1	39
.85- .90	300	22 ± 13	10 ± 9	13	35 ± 2	15	38 ± 4	0 ± 1	10
.90- .98	332	21 ± 10	2 ± 8	62	23 ± 1	75	23 ± 3	0 ± 0	62
.98-1.1	277	27 ± 6	-13 ± 5	43	11 ± 1	7	7 ± 2	1 ± 0	31
1.1 -1.2	258	15 ± 13	- 3 ± 12	42	12 ± 1	55	12 ± 2	0 ± 0	42
1.2 -1.3	333	4 ± 32	13 ± 28	9	19 ± 1	14	18 ± 4	0 ± 0	8

Table IV. Results of fits of the "σ" data points, for Experiment 1 in $\pi^+ p \to (\pi^+\pi^-)\Delta^{++}(1238)$, to the assumed forms a and a + bt.

		"σ" = a		"σ" = a + bt		
$\pi^+\pi^-$ Mass Range (GeV)	Events	σ (mb)	Prob. (%)	σ (mb)	$b\mu^2$ (mb)	Prob. (%)
.28- .45	61	11 ± 1	16	6 ± 3	1 ± 1	86
.45- .55	98	27 ± 3	1	25 ± 7	0 ± 1	< 1
.55- .63	159	38 ± 3	50	44 ± 8	-1 ± 1	45
.63- .68	152	43 ± 4	60	32 ± 10	2 ± 1	71
.68- .72	237	78 ± 5	17	112 ± 17	-4 ± 2	50
.72- .75	233	84 ± 6	3	111 ± 17	-3 ± 2	5
.75- .78	288	113 ± 7	70	104 ± 21	1 ± 3	62
.78- .81	258	115 ± 7	< 1	152 ± 27	-4 ± 3	< 1
.81- .84	217	79 ± 5	77	83 ± 18	0 ± 2	69
.84- .88	209	60 ± 4	1	95 ± 17	-3 ± 1	5
.88- .95	194	37 ± 3	74	30 ± 11	1 ± 1	65
.95-1.05	139	23 ± 2	3	45 ± 12	-2 ± 1	7

Table V. Results of fits of the "σ" data points, for Experiment 2 in $\pi^+ p \rightarrow (\pi^+\pi^-)\Delta^{++}(1238)$, to the assumed forms a and a + bt.

		"σ" = a		"σ" = a + bt		
$\pi^+\pi^-$ Mass Range (GeV)	Events	σ (mb)	Prob. (%)	σ (mb)	$b\mu^2$	Prob. (%)
.40- .60	110	24 ± 3	1	3 ± 7	6 ± 2	95
.60- .68	120	44 ± 4	50	25 ± 14	4 ± 3	99
.68- .72	147	81 ± 7	9	47 ± 22	5 ± 3	15
.72- .75	160	125 ± 10	8	97 ± 30	4 ± 4	6
.75- .78	182	143 ± 11	28	112 ± 33	4 ± 4	25
.78- .81	163	143 ± 11	55	190 ± 47	-6 ± 6	58
.81- .86	198	71 ± 5	< 1	40 ± 19	4 ± 2	< 1
.86- .96	201	38 ± 3	20	15 ± 11	2 ± 1	62
.96-1.16	163	20 ± 2	1.5	22 ± 6	0 ± 0	< 1

Table VI. Results of fits of the "σ" data points, for Experiment 3 in $\pi^+ p \rightarrow (\pi^+\pi^-)\Delta^{++}(1238)$, to the assumed forms a and a + bt.

		"σ" = a		"σ" = a + bt		
$\pi^+\pi^-$ Mass Range (GeV)	Events	σ (mb)	Prob. (%)	σ (mb)	$b\mu^2$ (mb)	Prob. (%)
.40- .61	122	29 ± 3	< 1	2 ± 8	11 ± 3	52
.61- .71	199	68 ± 5	26	52 ± 13	4 ± 3	30
.71- .75	210	148 ± 10	35	101 ± 30	12 ± 7	55
.75- .78	183	129 ± 10	< 1	127 ± 24	0 ± 5	< 1
.78- .82	205	123 ± 9	6	155 ± 29	-7 ± 6	5
.82- .88	211	79 ± 6	9	86 ± 16	-1 ± 3	6
.88-1.0	231	33 ± 2	< 1	14 ± 7	4 ± 1	1
1.0 -1.18	215	18 ± 1	46	13 ± 5	1 ± 1	52
1.18-1.32	256	27 ± 2	62	26 ± 6	0 ± 1	50
1.32-1.62	218	12 ± 1	4	25 ± 4	-1 ± 1	86

Table VII. Extrapolated $\pi^+\pi^-$ elastic scattering cross-sections, averaged over the three experiments (in mb).

$\pi^-p \to (\pi^-\pi^+)n$				$\pi^+p \to (\pi^+\pi^-)\Delta^{++}(1238)$		
$\pi^+\pi^-$ mass range (GeV)	"$t\sigma$"=a+bt	"$t\sigma$"=bt	"$t\sigma$"=bt+ct^2	$\pi^+\pi^-$ mass range (GeV)	"σ"=a	"σ"=a+bt
0.28 - 0.46	40 ± 8[h]	14 ± 1[h]	5 ± 3[h]	0.28 - 0.45	11 ± 1[g]	6 ± 3[g]
0.46 - 0.54	24 ± 8	27 ± 2	24 ± 4	0.45 - 0.55	27 ± 3[g]	25 ± 7[g]
0.54 - 0.62	45 ± 7	32 ± 2	25 ± 3	0.55 - 0.60	35 ± 3[g]	40 ± 7[g]
0.62 - 0.68	39 ± 8	46 ± 2	45 ± 4	0.60 - 0.68	43 ± 2	38 ± 7
0.68 - 0.72	79 ± 12	76 ± 3	76 ± 6	0.68 - 0.72	79 ± 4[h]	88 ± 14[h]
0.72 - 0.75	104 ± 15	105 ± 4	106 + 8	0.72 - 0.75	106 ± 5	107 ± 13
0.75 - 0.78	132 ± 16	111 ± 4	93 ± 7	0.75 - 0.78	124 ± 5	114 ± 14
0.78 - 0.81	116 ± 16	97 ± 3	85 ± 6	0.78 - 0.81	123 ± 5	159 ± 18
0.81 - 0.85	69 ± 12	63 ± 2	61 ± 4	0.81 - 0.84	87 ± 4	90 ± 12
0.85 - 0.90	34 ± 10	39 ± 1	36 ± 3	0.84 - 0.88	62 ± 3	66 ± 8
0.90 - 0.98	34 ± 8[h]	24 ± 1[h]	21 ± 2[h]	0.88 - 0.96	36 ± 2	19 ± 5
0.98 - 1.1	28 ± 5[h]	12 ± 1[h]	7 ± 1[h]	0.96 - 1.18	19 ± 1[h]	17 ± 4[h]
1.1 - 1.2	20 ± 12[h]	13 ± 1[h]	12 ± 2[h]	1.18 - 1.32	27 ± 2[g]	26 ± 6[g]
1.2 - 1.3	4 ± 32[g]	19 ± 1[g]	18 ± 4[g]	1.32 - 1.60	12 ± 1[g]	25 ± 4[g]

g. based on one experiment

h. average of two experiments

FIGURE CAPTIONS

Fig. 1. Single-pion-exchange diagrams for the reactions considered in this paper.

Fig. 2. π^+p effective mass spectra for the reaction $\pi^+p \to \pi^+\pi^-\pi^+p$. Two combinations are plotted for each event.

Fig. 3. $\pi^+\pi^-$ effective mass spectra for the reaction $\pi^-p \to \pi^+\pi^-n$.

Fig. 4. $\pi^+\pi^-$ effective mass spectra for events of the type $\pi^+p \to \pi^+\pi^-(\pi^+p)$ where $1.12 < M(\pi^+p) < 1.34$ GeV. If both π^+p combinations fall within these limits we use that combination with the smallest t from the target proton to the π^+p system. One $\pi^+\pi^-$ combination is plotted for each event.

Fig. 5. The experimental "$t\sigma$" quantities for reaction (1a) and Experiment 1, defined in Eq. (7a), for all the 11 denoted $\pi^+\pi^-$ mass regions. The straight lines and the extrapolated points at $t = -\mu^2$ represent the expansion "$t\sigma$" = a + bt using for a and b the best fit values obtained in the least-squares fits.

Fig. 6. The experimental "$t\sigma$" quantities for reaction (1a) and Experiment 2, defined in Eq. (7a), for the 13 denoted $\pi^+\pi^-$ mass regions. The straight lines and the extrapolated points at $t = -\mu^2$ represent the expansion "$t\sigma$" = a + bt using for a and b the best fit values obtained in the least-squares fits.

Fig. 7. The experimental "$t\sigma$" quantities for reaction (1a) and Experiment 3, defined in Eq. (7a), for the 13 denoted $\pi^+\pi^-$ mass regions. The straight lines and the extrapolated points at $t = -\mu^2$ represent the expansion "$t\sigma$" = a + bt using for a and b the best fit values obtained in the least-squares fits.

Fig. 8. Extrapolated on-mass-shell $\pi^+\pi^-$ elastic scattering cross sections, obtained in least-squares fits of the "$t\sigma$" points shown in Figs. 5-7 to the assumed forms bt, a + bt, and bt + ct^2, plotted as a function of $\pi^+\pi^-$ effective mass. The curves are $12\pi\lambda\!\!\!^-{}^2$ which is the unitarity limit for an elastic p-wave $\pi\pi$ resonance.

Fig. 9. The experimental "σ" quantities for reaction (1b) and Experiment 1, defined in Eq. (7b), for the 12 denoted $\pi^+\pi^-$ mass regions. The straight lines and the extrapolated cross sections at $t = -\mu^2$ represent the expansion "σ" = a + bt using for a and

b the best fit values obtained in the least-squares fits.

Fig. 10. The experimental "σ" quantities for reaction (1b) and Experiment 2, defined in Eq. (7b), for the 9 denoted $\pi^+\pi^-$ mass regions. The straight lines and the extrapolated cross sections at $t = -\mu^2$ represent the expansion "σ" = a + bt using for a and b the best fit values obtained in the least-squares fits.

Fig. 11. The experimental "σ" quantities for reaction (1b) and Experiment 3, defined in Eq. (7b), for the 10 denoted $\pi^+\pi^-$ mass regions. The straight lines and the extrapolated cross sections at $t = -\mu^2$ represent the expansion "σ" = a + bt using for a and b the best fit values obtained in the least-squares fits.

Fig. 12. Extrapolated on-mass-shell $\pi^+\pi^-$ elastic scattering cross sections, obtained in least-squares fits of the "σ" points shown in Figs. 9-11 to the assumed forms a and a + bt, plotted as a function of $\pi^+\pi^-$ effective mass. The curves are $12\pi\lambda\!\!\!^{-2}$ which is the unitarity limit for an elastic p-wave $\pi\pi$ resonance.

Fig. 13. Extrapolated on-mass-shell $\pi^+\pi^-$ elastic scattering cross sections, averaged over the three center-of-mass energy regions (or experiments). The solid and dashed curves represent the "up-up" and "up-down" solution values for δ_0^0, respectively, in the expansion (8).

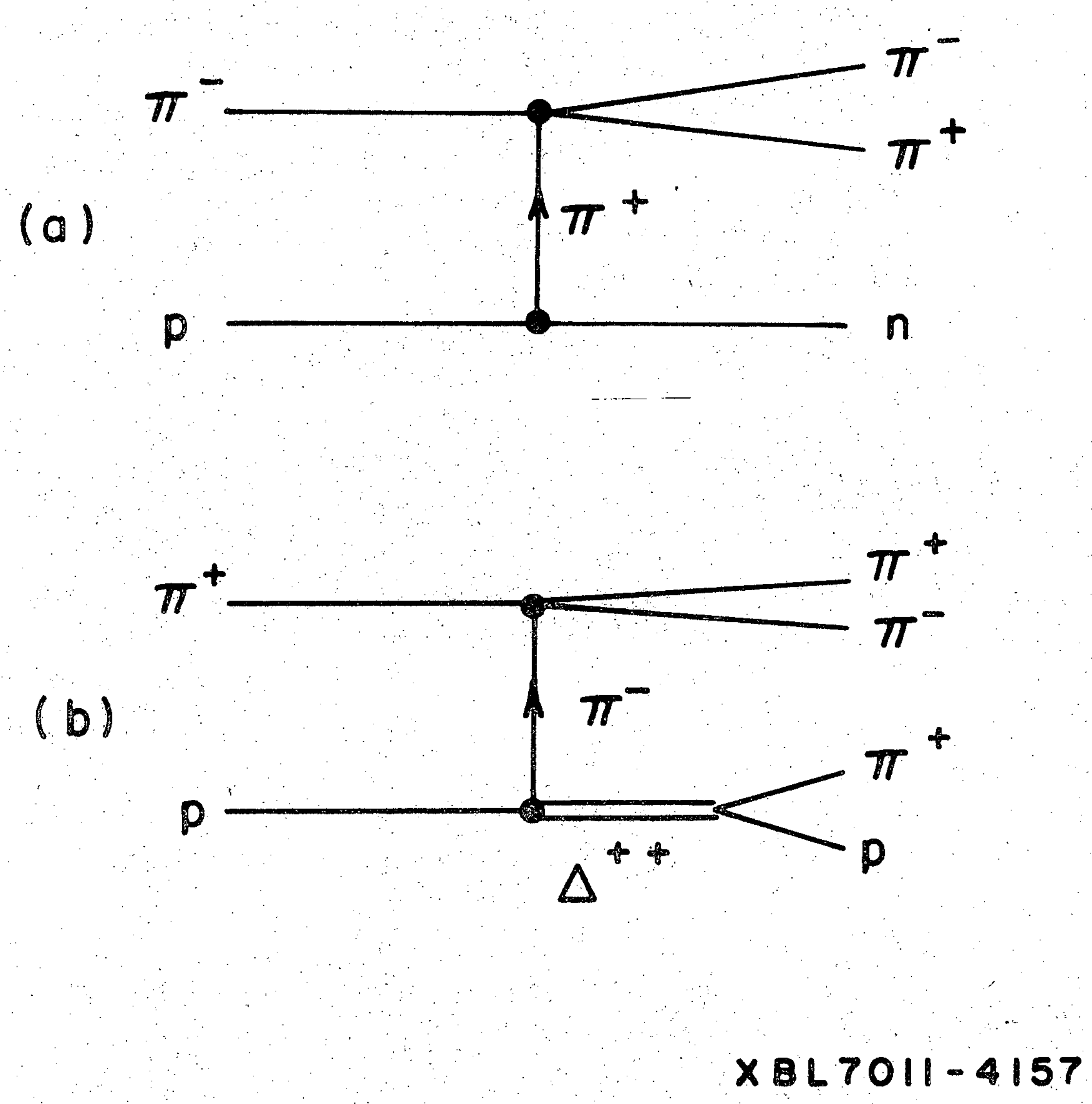

FIGURE 1

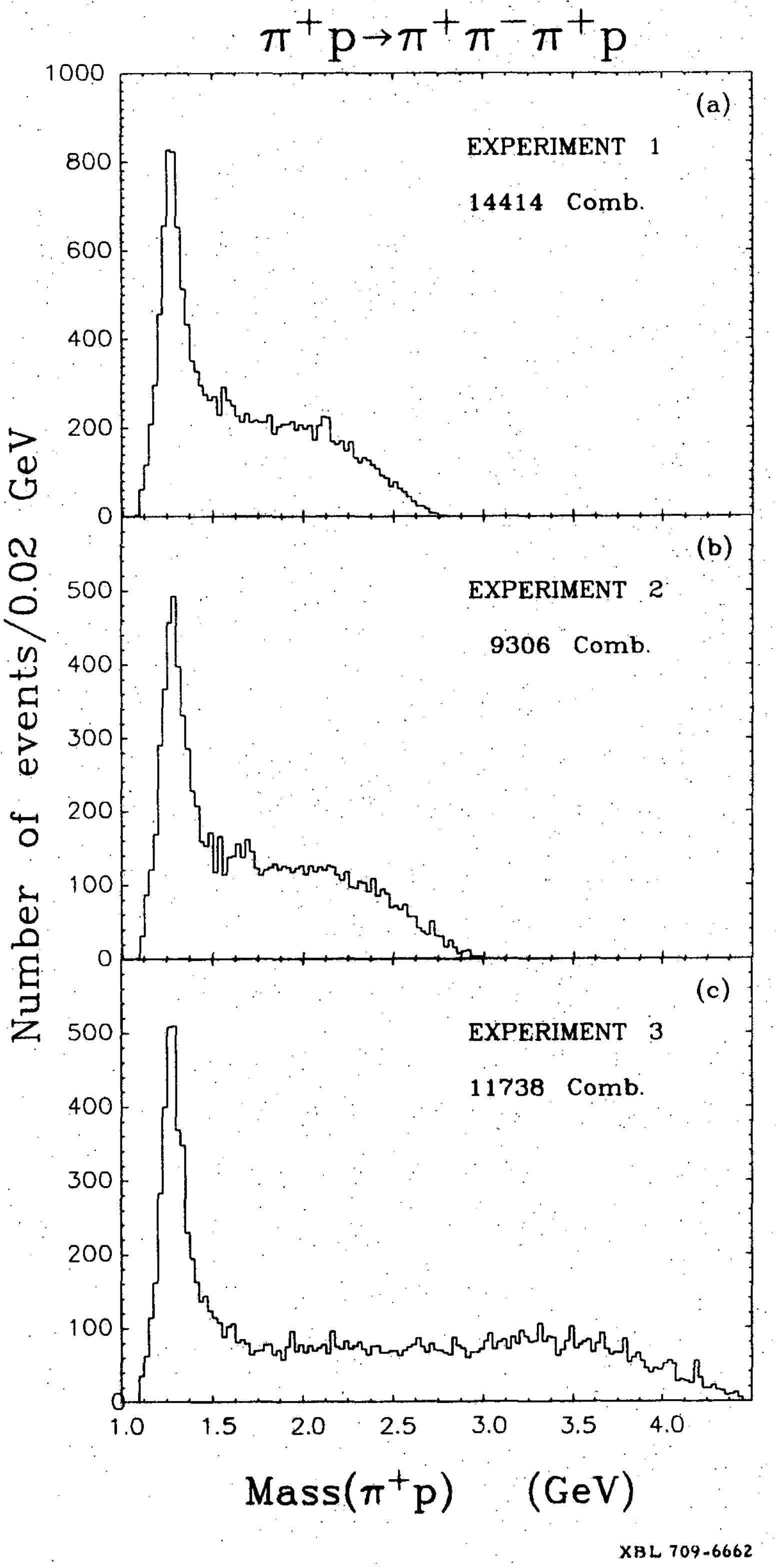

$\pi^+p\rightarrow\pi^+\pi^-\pi^+p$
(a)
EXPERIMENT 1
14414 Comb.
(b)
EXPERIMENT 2
9306 Comb.
(c)
EXPERIMENT 3
11738 Comb.
Number of events/0.02 GeV
1000
800
600
400
200
0
500
400
300
200
100
0
500
400
300
200
100
0
1.0
1.5
2.0
2.5
3.0
3.5
4.0
Mass(π^+p) (GeV)
XBL 709-6662

FIGURE 2

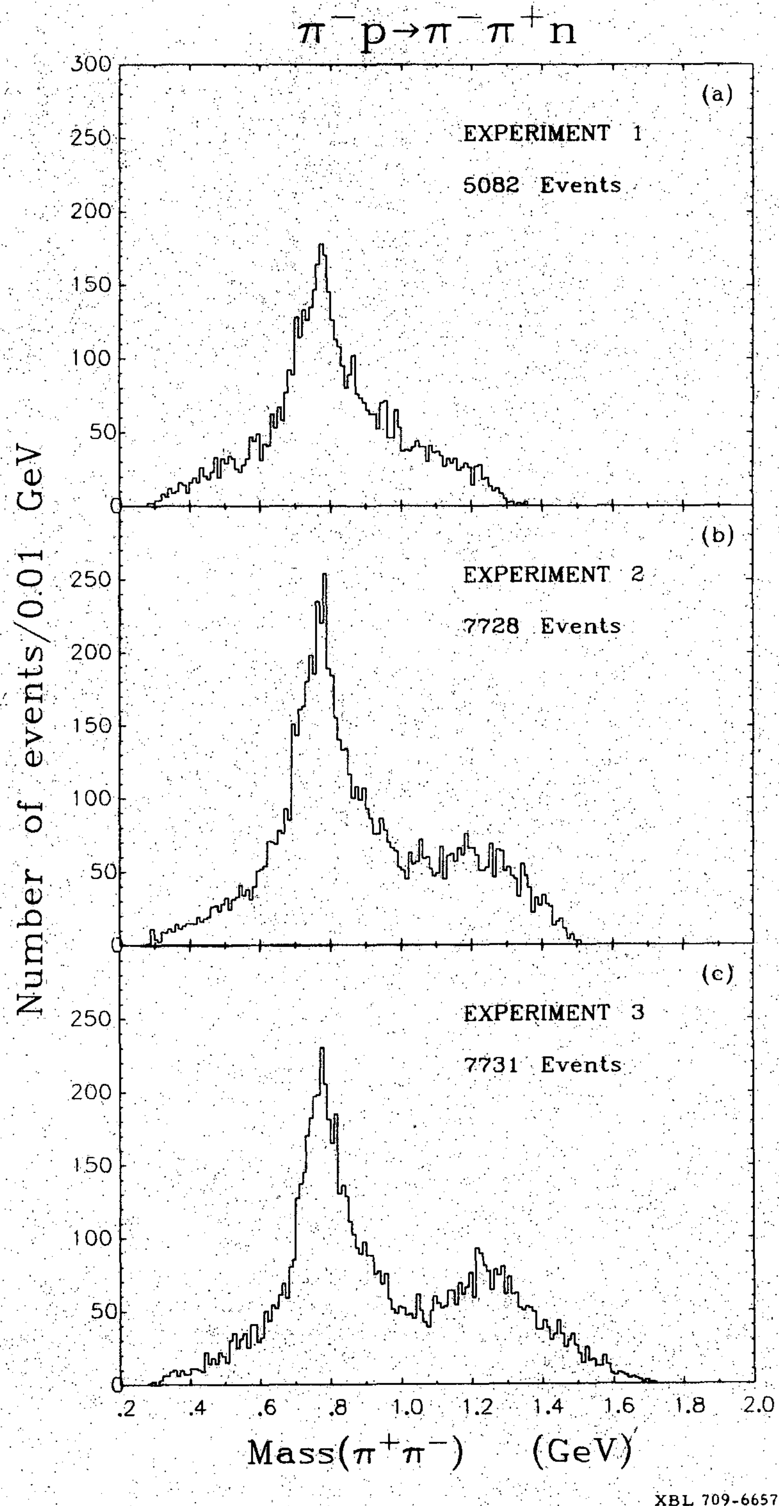

$\pi^- p \to \pi^- \pi^+ n$
(a)
EXPERIMENT 1
5082 Events
(b)
EXPERIMENT 2
7728 Events
(c)
EXPERIMENT 3
7731 Events
Number of events/0.01 GeV
Mass($\pi^+\pi^-$) (GeV)
300
250
200
150
100
50
0
.2
.4
.6
.8
1.0
1.2
1.4
1.6
1.8
2.0
XBL 709-6657

FIGURE 3

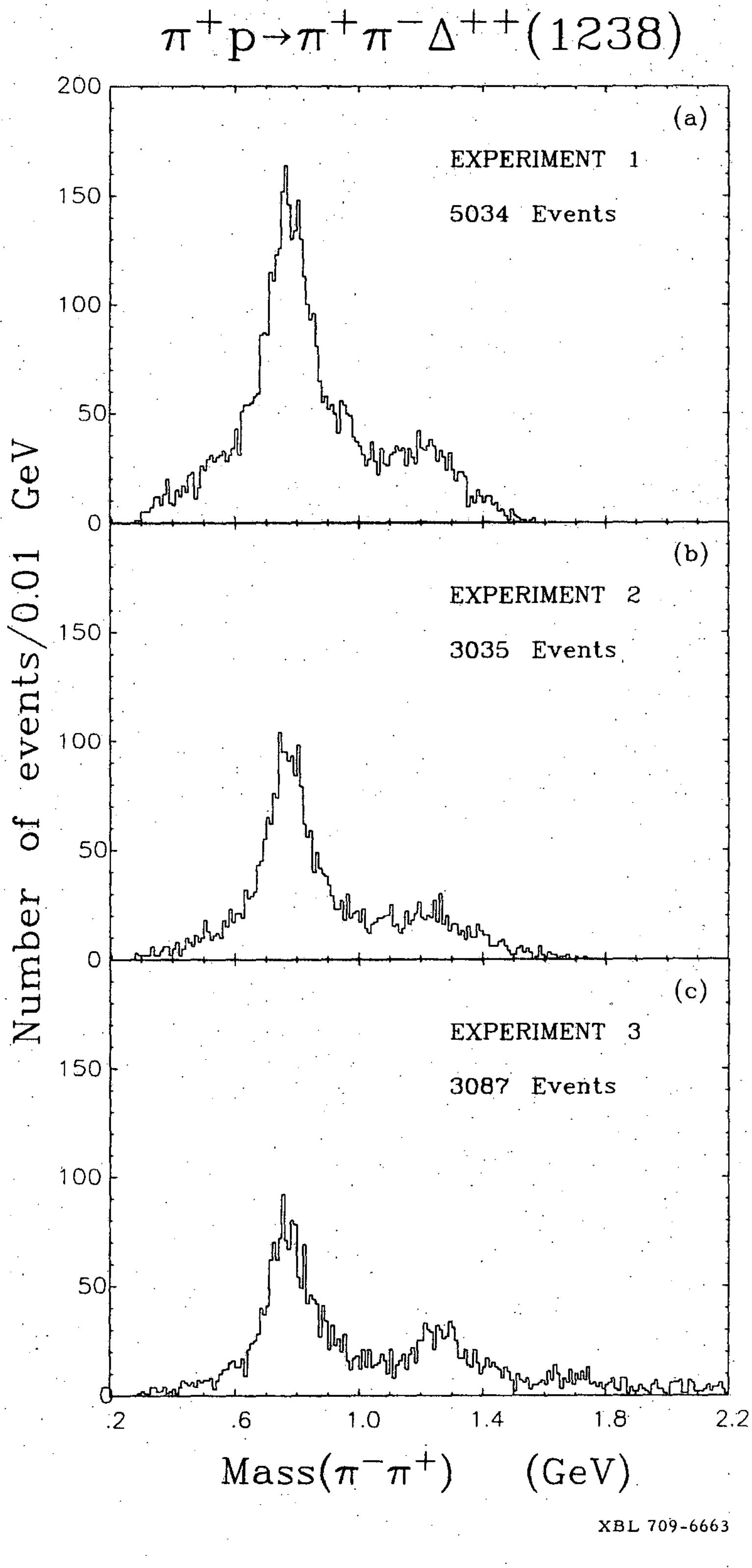

$\pi^+p\rightarrow\pi^+\pi^-\Delta^{++}(1238)$
(a)
EXPERIMENT 1
5034 Events
(b)
EXPERIMENT 2
3035 Events
(c)
EXPERIMENT 3
3087 Events
Number of events/0.01 GeV
200
150
100
50
0
.2
.6
1.0
1.4
1.8
2.2
Mass($\pi^-\pi^+$) (GeV)
XBL 709-6663

FIGURE 4

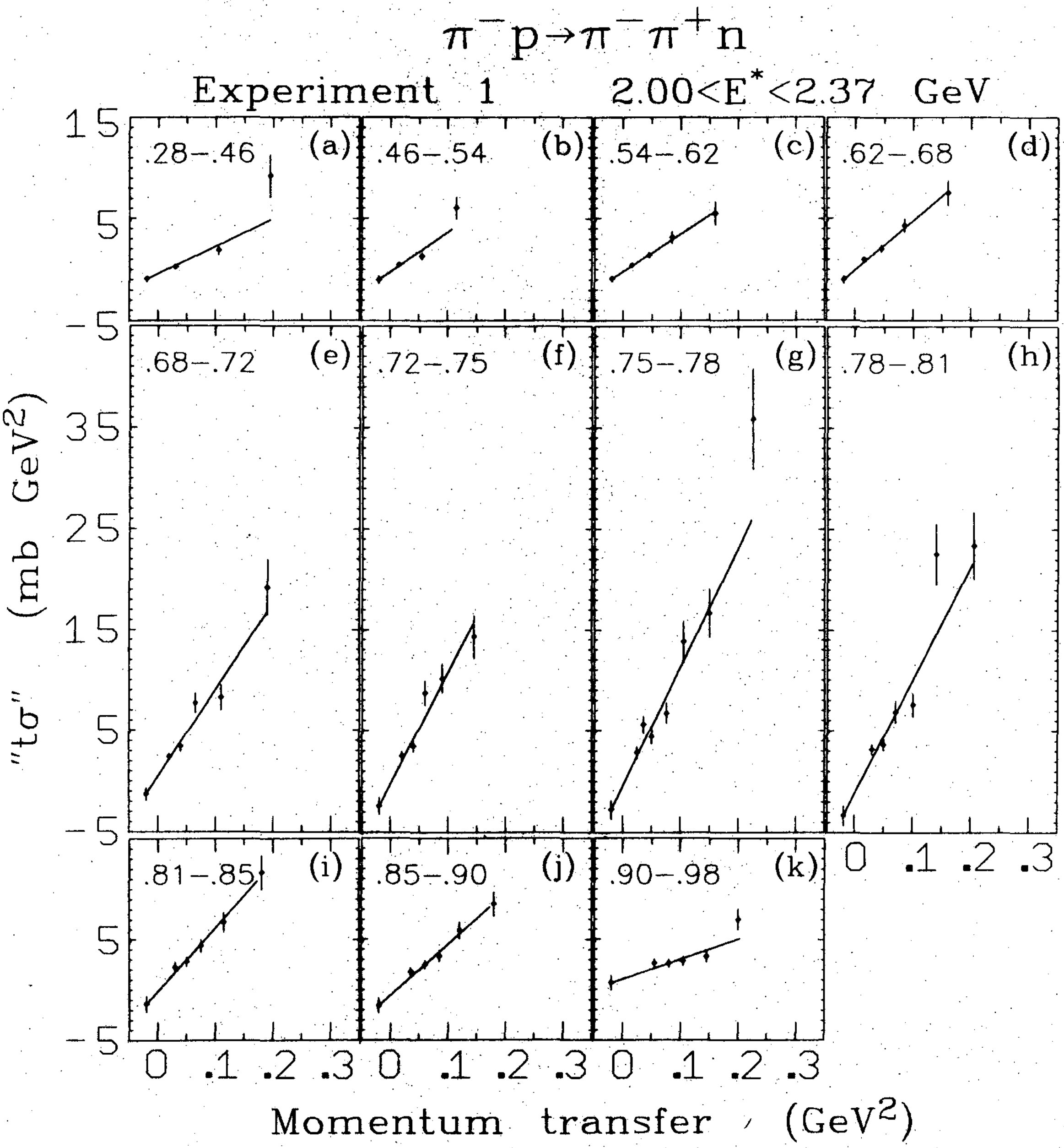

XBL 709-6656

FIGURE 5

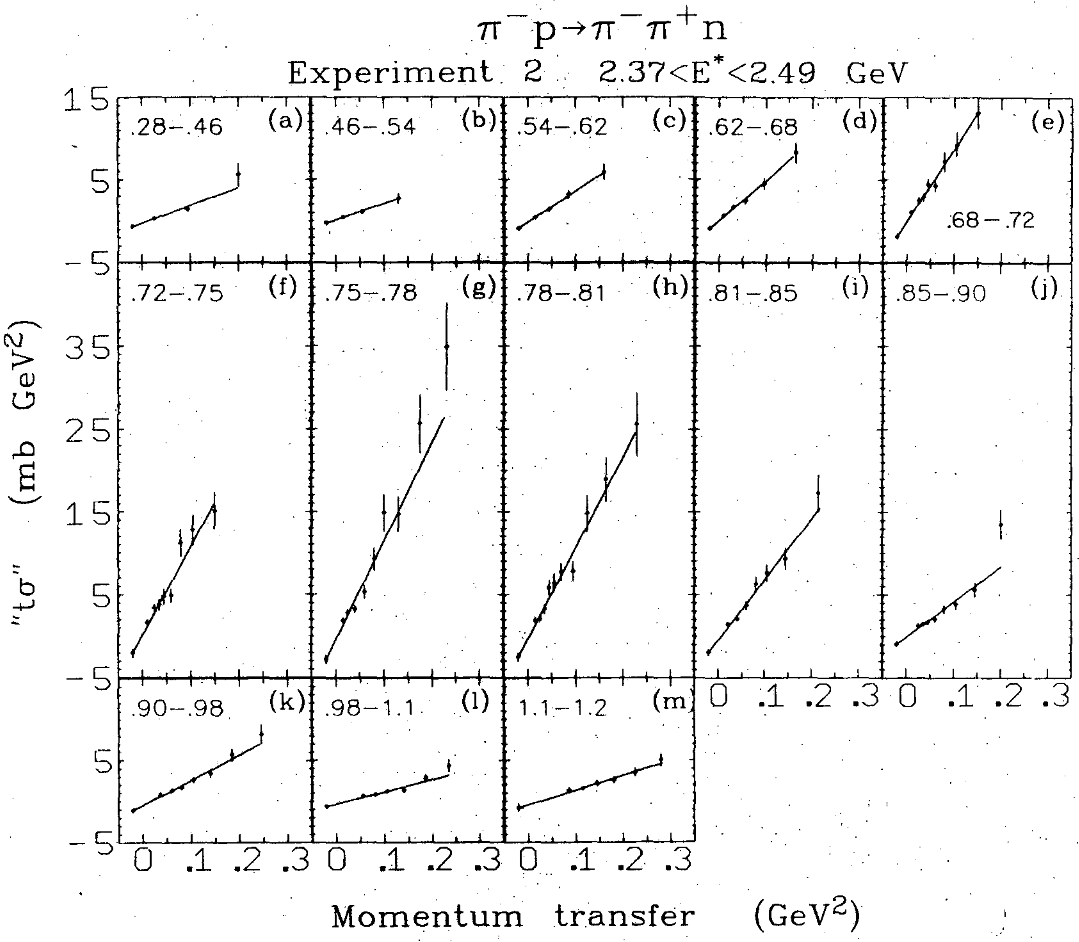

$\pi^- p \to \pi^- \pi^+ n$
Experiment 2 $2.37 < E^* < 2.49$ GeV
.28–.46 (a)
.46–.54 (b)
.54–.62 (c)
.62–.68 (d)
(e) .68–.72
.72–.75 (f)
.75–.78 (g)
.78–.81 (h)
.81–.85 (i)
.85–.90 (j)
.90–.98 (k)
.98–1.1 (l)
1.1–1.2 (m)
"tσ" (mb GeV^2)
Momentum transfer (GeV^2)
XBL 709-6659

FIGURE 6

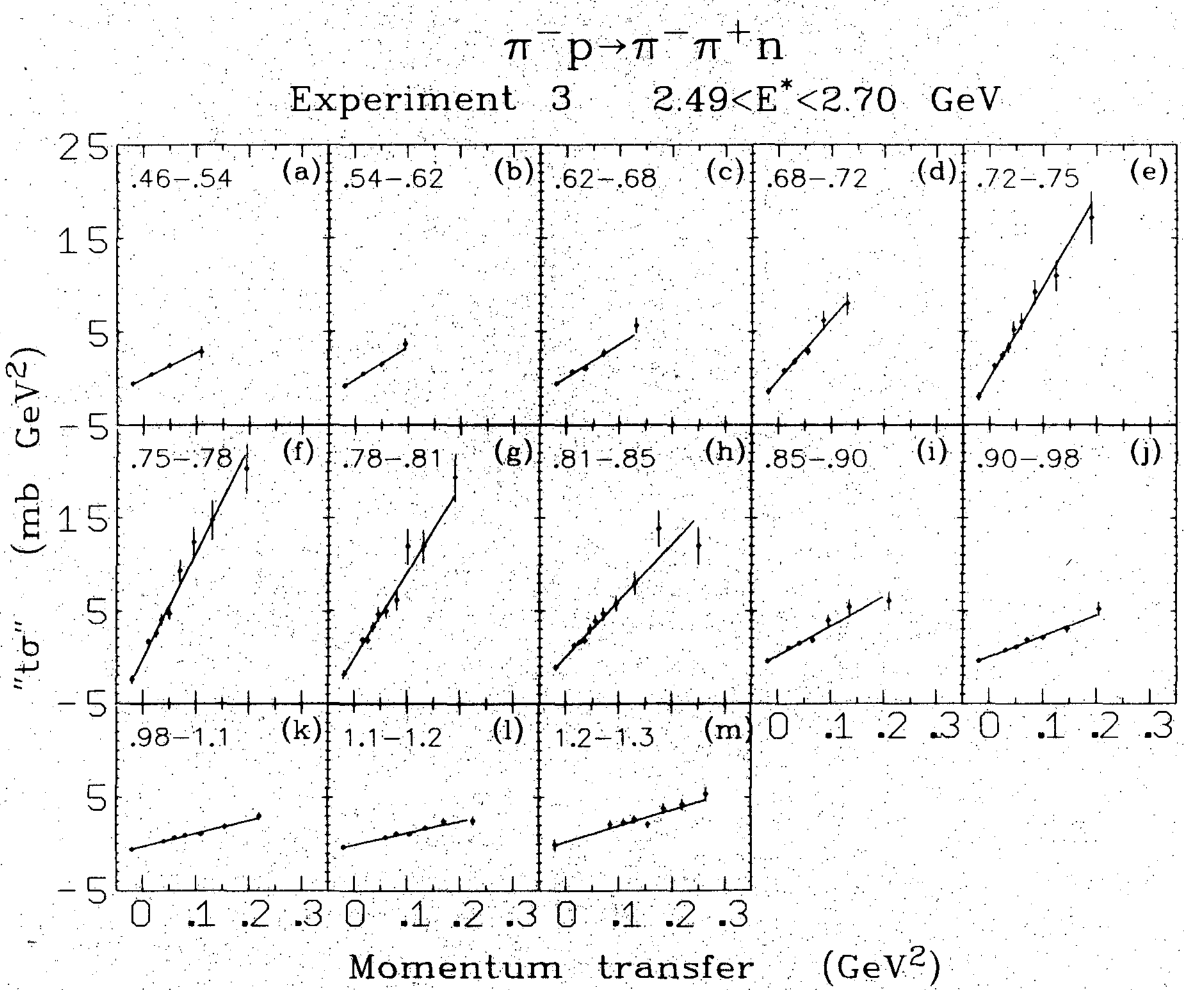

XBL 709-6654

FIGURE 7

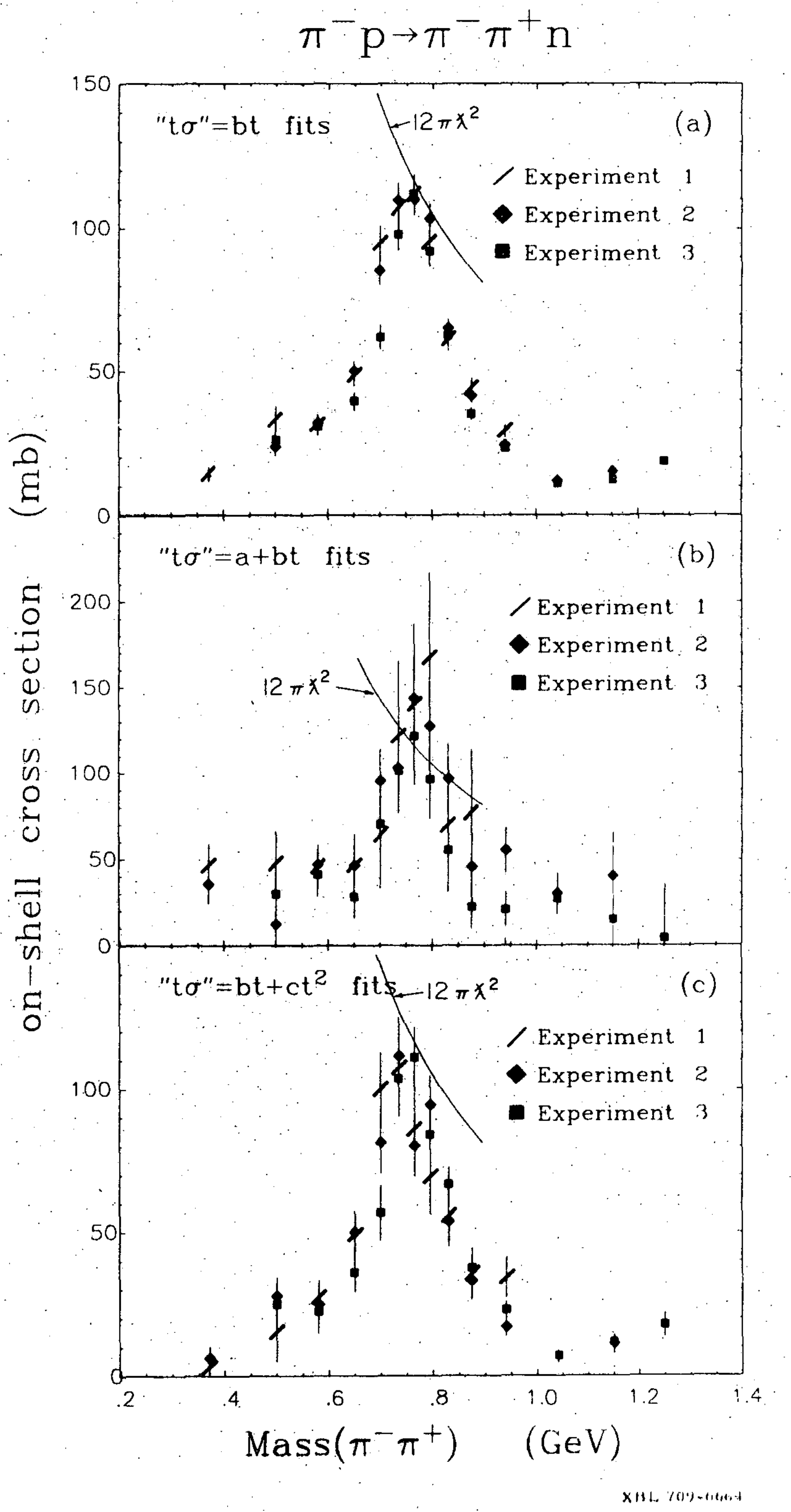

$\pi^- p \to \pi^- \pi^+ n$
"tσ"=bt fits
(a)
$12\pi\lambda^2$
Experiment 1
Experiment 2
Experiment 3
"tσ"=a+bt fits
(b)
"tσ"=bt+ct² fits
(c)
on-shell cross section (mb)
Mass($\pi^-\pi^+$) (GeV)
XBL 709-6664

FIGURE 8

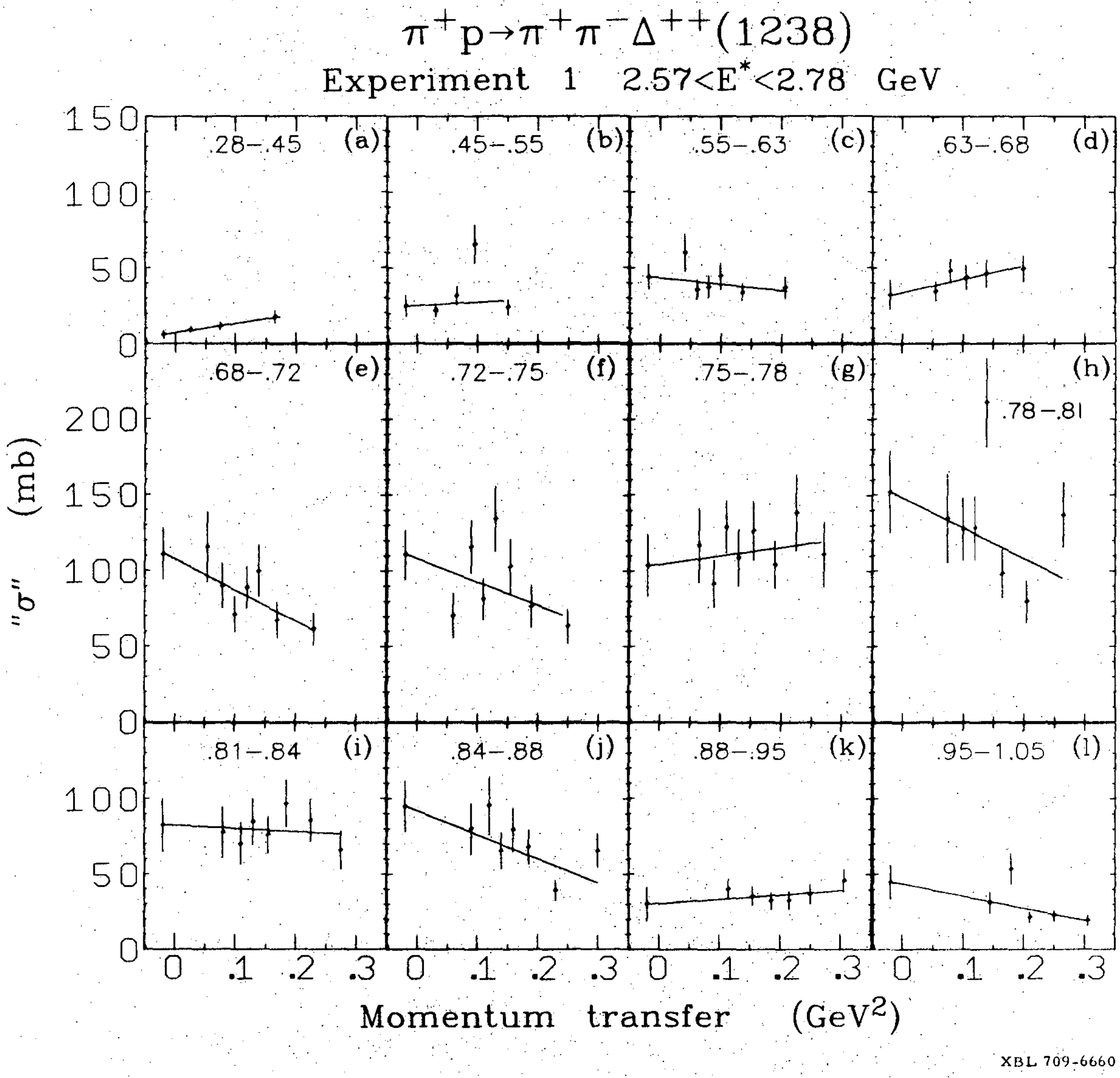
$\pi^+p\to\pi^+\pi^-\Delta^{++}(1238)$
Experiment 1 2.57<E*<2.78 GeV
.28–.45 (a)
.45–.55 (b)
.55–.63 (c)
.63–.68 (d)
.68–.72 (e)
.72–.75 (f)
.75–.78 (g)
(h) .78–.81
.81–.84 (i)
.84–.88 (j)
.88–.95 (k)
.95–1.05 (l)
"σ" (mb)
Momentum transfer (GeV²)
XBL 709-6660

FIGURE 9

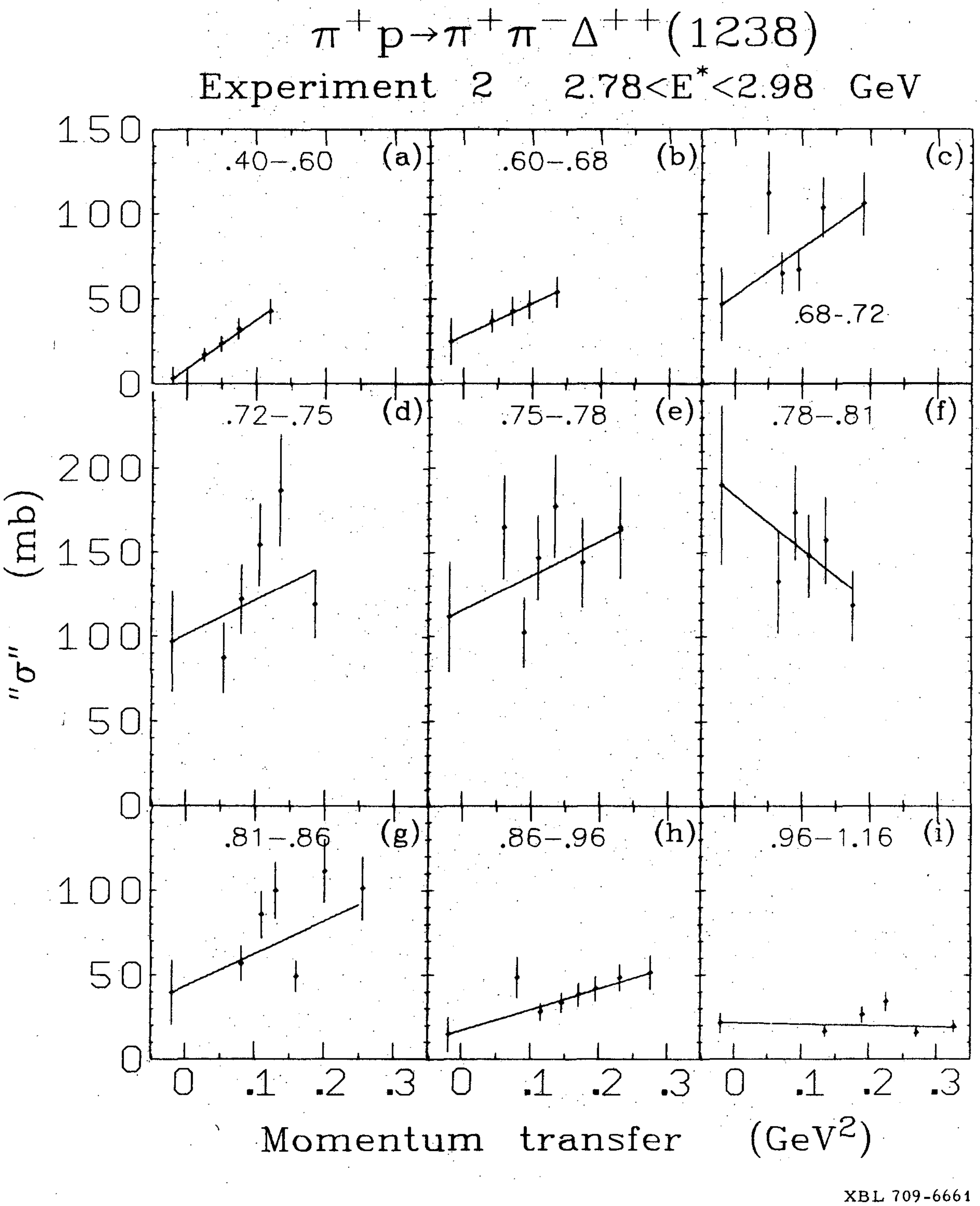
π⁺p→π⁺π⁻Δ⁺⁺(1238)
Experiment 2 2.78<E*<2.98 GeV
.40–.60 (a)
.60–.68 (b)
(c) .68-.72
.72–.75 (d)
.75–.78 (e)
.78–.81 (f)
.81–.86 (g)
.86–.96 (h)
.96–1.16 (i)
"σ" (mb)
Momentum transfer (GeV2)
150 100 50 0 200 150 100 50 0 100 50 0
0 .1 .2 .3
XBL 709-6661

FIGURE 10

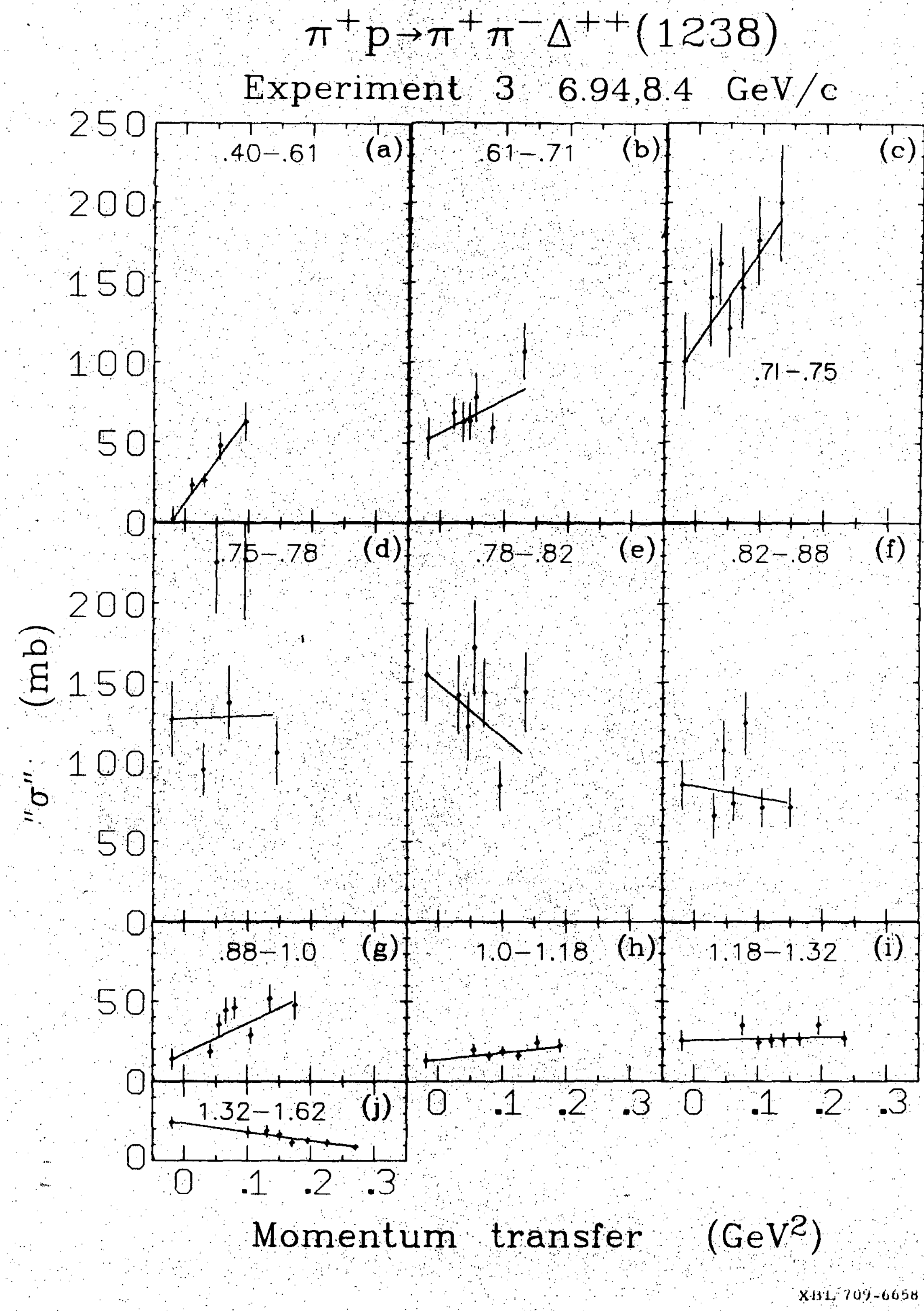
$\pi^+ p \to \pi^+ \pi^- \Delta^{++}(1238)$
Experiment 3 6.94,8.4 GeV/c
.40–.61
(a)
.61–.71
(b)
(c)
.71–.75
.75–.78
(d)
.78–.82
(e)
.82–.88
(f)
.88–1.0
(g)
1.0–1.18
(h)
1.18–1.32
(i)
1.32–1.62
(j)
"σ" (mb)
0
50
100
150
200
250
0
.1
.2
.3
Momentum transfer (GeV^2)
XBL 709-6658

FIGURE 11

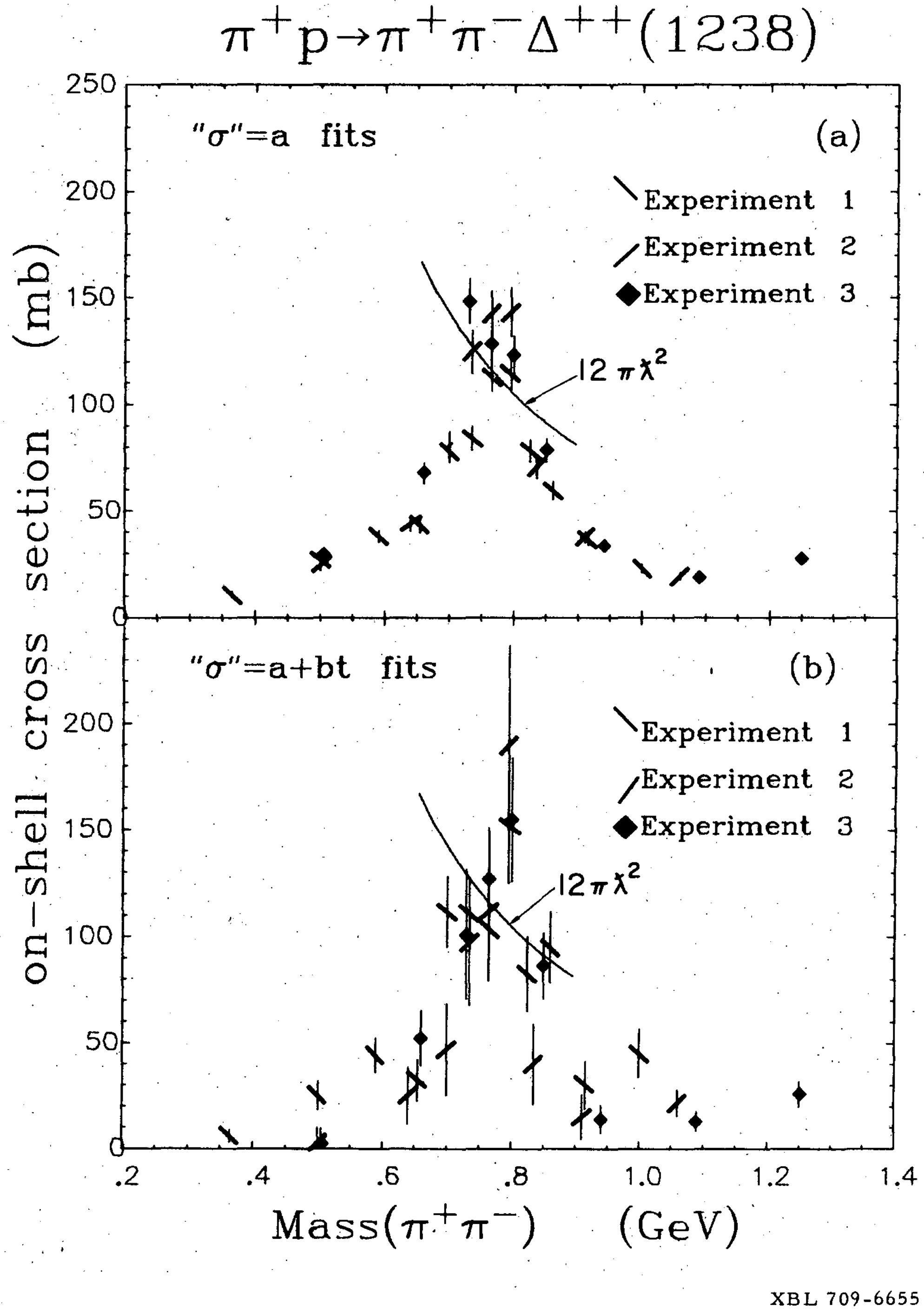
π⁺p→π⁺π⁻Δ⁺⁺(1238)
"σ"=a fits
(a)
Experiment 1
Experiment 2
Experiment 3
12πƛ²
"σ"=a+bt fits
(b)
on-shell cross section (mb)
Mass(π⁺π⁻) (GeV)
XBL 709-6655

FIGURE 12

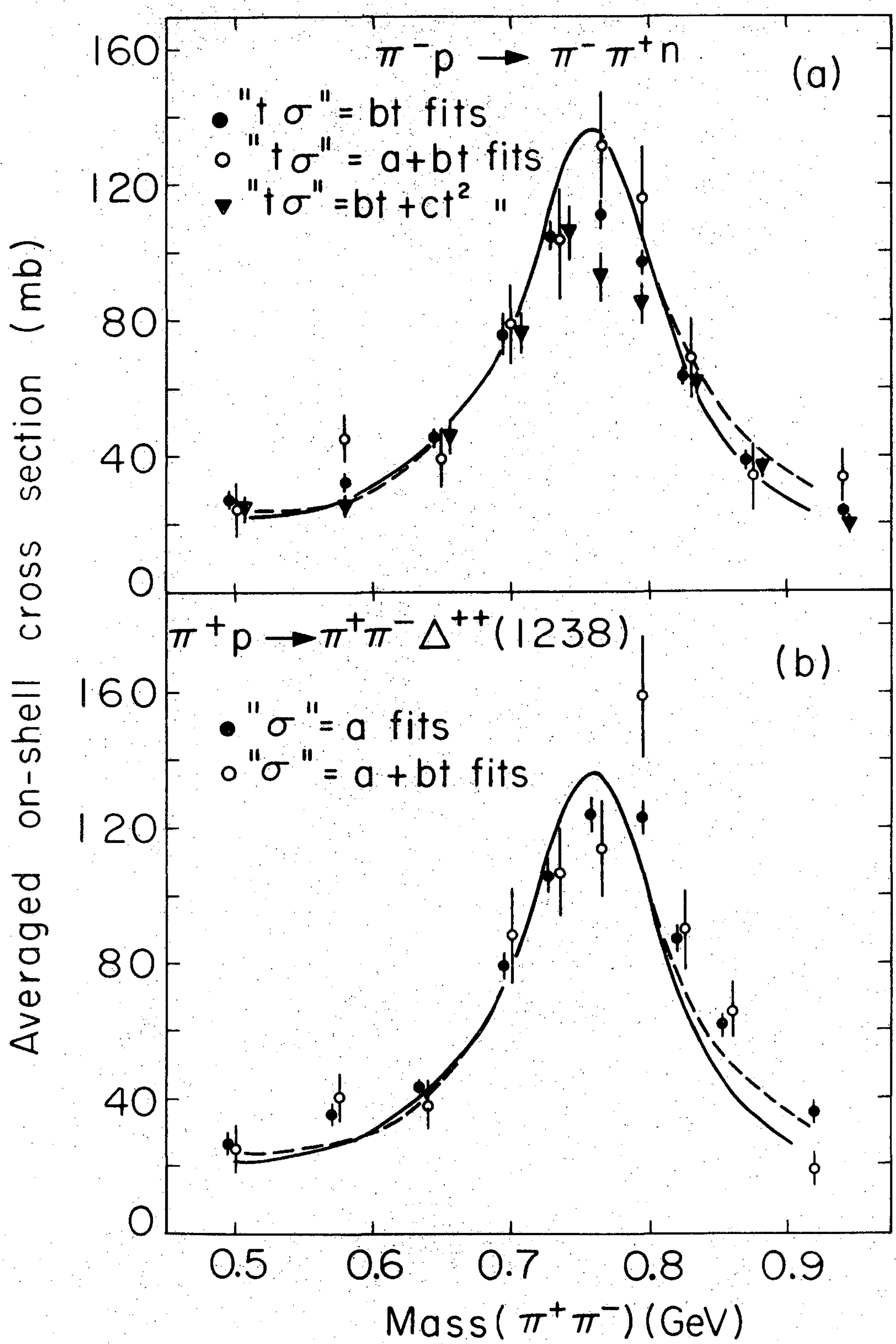

XBL7011-4156

FIGURE 13

TECHNICAL INFORMATION DIVISION
LAWRENCE RADIATION LABORATORY
UNIVERSITY OF CALIFORNIA
BERKELEY, CALIFORNIA 94720